Coherent Microwave Marine Radar Measurements of Directional Ocean Wave Spectra and Mean Radial Current Fields

Dennis B Trizna,
Imaging Science Research, Inc
6103 Virgo Court
Burke, VA 22015

Abstract- **Results of measurements of ocean waves using a coherent marine radar are presented. Data were collected in a coastal environment, at the U.S. Army Corps of Engineers Field Research Facility, Duck, N.C. Measurements of ocean wave spectra derived from maps of radial components of orbital wave velocity are used to measure directional ocean wave spectra, using three-dimensional FFT algorithms. Wave height spectra can be derived directly from such measurements, without the need for a modulation transfer function (MTF) that is used for traditional marine radars. The MTF approaches can suffer from wind speed variability and wind-wave relative direction effects, and are typically robust only for equilibrium wind-wave conditions. A discussion is presented of how one might use such data to provide a real time wave profile map of the coverage area. Such a map of wave height profiles is useful in ship motion response prediction for real-time applications such as safe helicopter landings under high sea conditions.**

I. INTRODUCTION

Marine radars have proven to be a useful tool in remote sensing of coastal ocean wave spectrum measurement and bathymetric morphology. This radar uses its capability to map ocean wave fields by means of the enhanced ocean backscatter intensity that occur near wave crests, with images generated by successive consecutive rotations, as a spatial-temporal data source. A general discussion of the methods that are used is provided here as an introduction to our application of them to coherent radar data.

A 10-minute sequence of echo intensity images when simply summed over all rotations provides a bathymetric estimate of offshore bar location as a result of mean echo enhancement due to localized wave breaking over the bars. Equivalent methods may be used with video camera images from rather high towers, which traced white water brightening of the imagery due to the enhanced breaking. However, there are limitations to this optical approach due to optimal solar illumination angle and lack of data during the night, whereas the radar data are available 24 hrs a day and illumination quality is not an issue.

Using 3D-FFT spectral analysis of the sub-windows of time-sequential imagery, and the dispersion relationship for ocean waves in shallow water, maps of general bathymetry can be generated over the area covered by the entire radar image. Measurement of the intensity of radar spectral peaks at discrete locations in the K_x, K_y plane generated for each frequency correspond to ocean wave spectral peaks in K-radius and azimuthal location. However, the spectral peak of the echo power must be related empirically to that of the ocean wave spectrum for each frequency by means of a scaling function, referred to as the Modulation Transfer Function (MTF). This empirical relationship is a function of several variables, such as wind direction relative to wave direction, presence of surfactant on the illuminated surface that suppresses the radar echo that can occur when onshore winds shift to offshore, and even offshore distance of the sub-windows used in the analysis.

NON-COHERENT STANDARD MARINE PRODUCT

Fig. 1 below shows the standard turn-key ISR output from processing code delivered with each system. Upper right is a single image of 512 collected each acquisition period (hour or half hour, as real time analysis is completed within a ten-minute period). The location of the windows that are clipped for 3D-FFT processing is shown as the red square lower right of the origin. Lower right shows an image of all 512

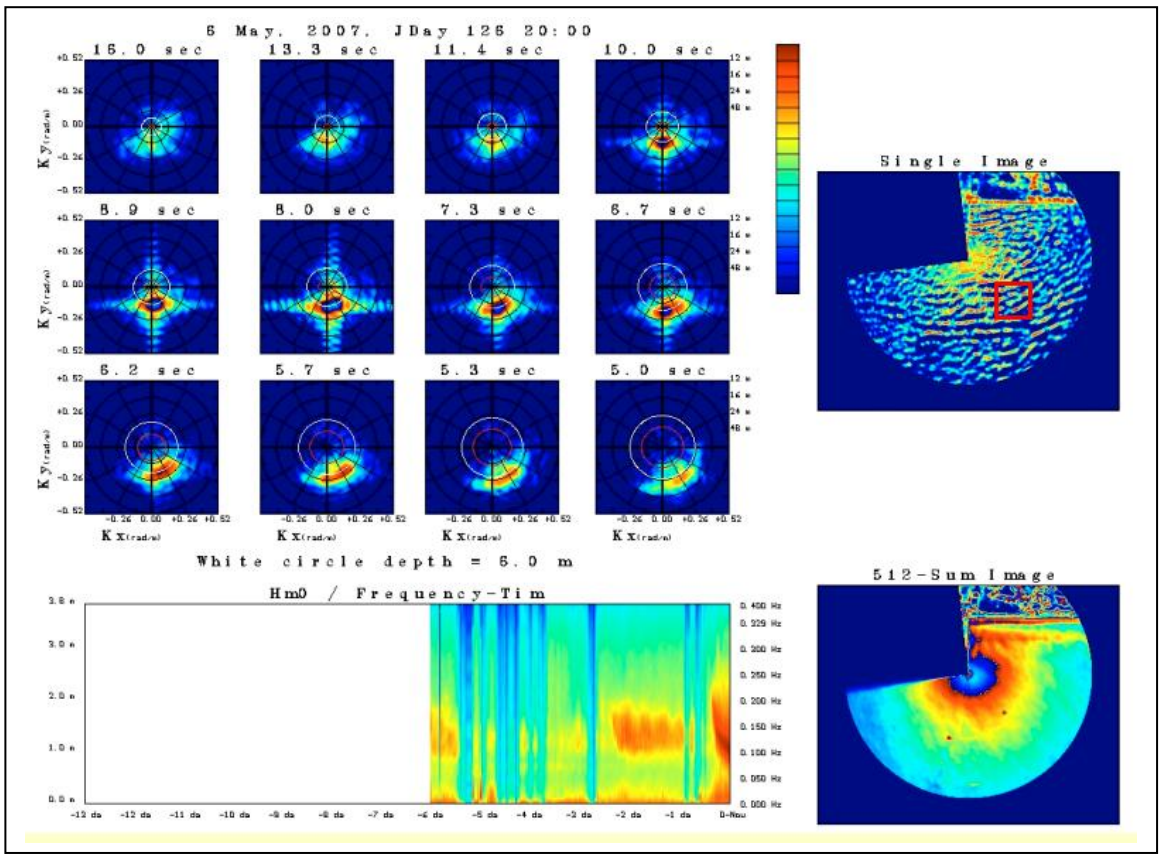

Fig.1. Standard product as describe in text, showing single rotation, sum of 512 rotations, 12 of 32 Kx-Ky spectra derived, and time spectrograph of frequency spectra covering up to 13 days with half-hour collections. Rips currents show in the sum image just as offshore bright jets that meander about when views in a time-sequence format.

rotations summed, and the location of the offshore bar is clearly seen, as well as several rip current jets.

At upper left are shown 12 user-selectable K_x-K_y spectra of 32 that are available. Dominant wave energy is seen in the 8-sec wave spectrum with the lightest blue center, given the wrapped spectrum color scheme. (dark blue to bright dark red covers 0-12.8 dB, then repeats to show 12.8 to 25.6 dB, and once again if waves are even higher). The red-lined square window in the single rotation image shows the size and location of the 64 x 64 pixel window extracted to use for 3D-FFT processing to produce the 32 frequency wave number spectra. The shallow water dispersion relation reflecting the hyperbolic tangent of depth times wave number is shown in each spectral plot as a yellow circle, one which the spectral peaks lie, confirming the mean depth at the sampling window. There is also a red circle drawn that reflects the deep water dispersion rule. Note that the longest 10-s waves are shore normal, a result of turning into shore in the shoaling process, while the highest frequency waves are closer to 30 deg north of normal, and are spread in angle compared to the longest waves.

The K-spectral peaks require a scaling factor, or MTF, to scale the radar echo spectral energy to ocean wave directional spectral energy, a different MTF derived for each frequency. The spectrograph at bottom left above reflects this MTF being applied, while the K-spectra above are raw radar echo spectra. We later show examples of how the MTF can be in error unless elements like wind-wave relative direction is accounted for, or atmospheric stability and low wind speed. Below about 5 m/s wind speed, the echo does decrease, as evidenced in the spectrograph when the background turns dark blue. Nonetheless, for high winds and waves when such wave information is important, the non-coherent marine radar offers a 24-hr data source that is relatively inexpensive and simple to deploy without fear of high waves tearing out instrumentation, as occurs for bottom mounted acoustic sensors and tethered buoys, for example.

A similar result collected during the same storm when the waves became higher and longer in wavelength is shown in Fig. 2 below for comparison. The waves have changed direction and two rip current features are visible in the 512-sum image to the right of the pier. The line running parallel to shore

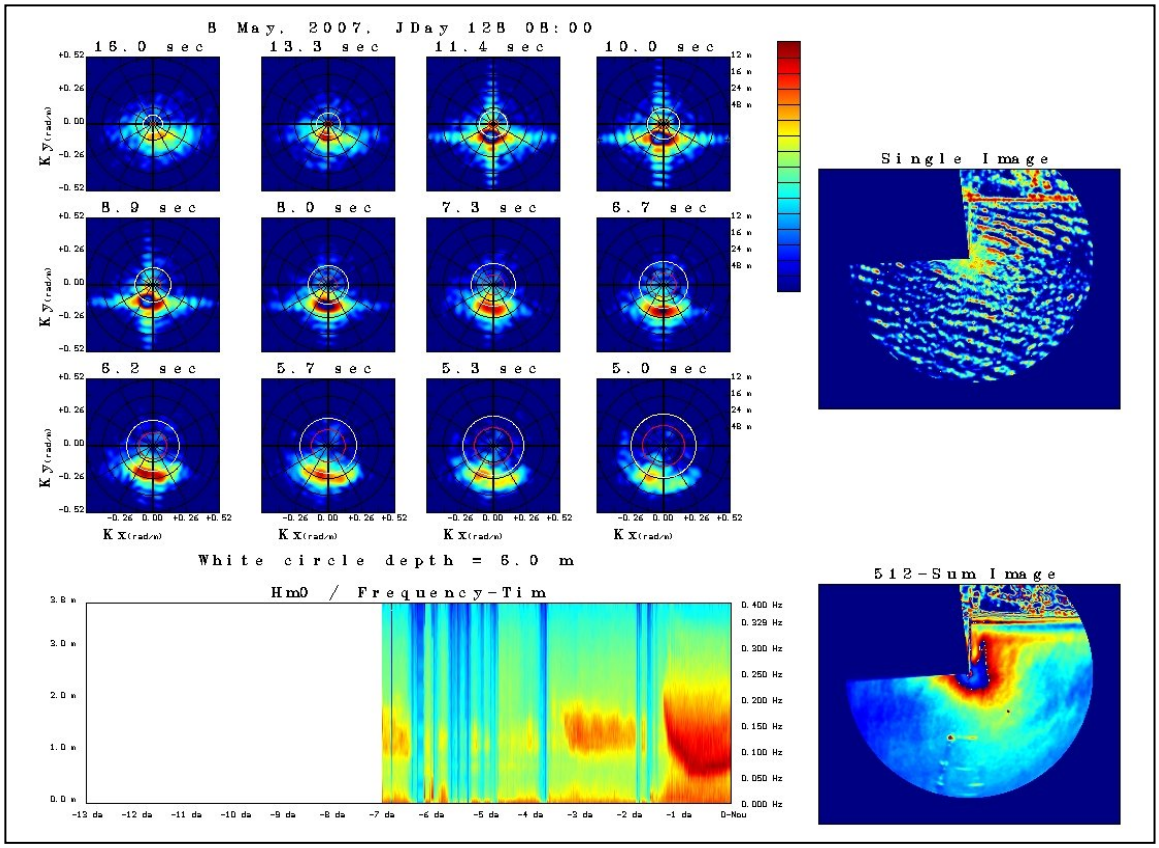

Fig. 2. A representation similar to the previous figure shows that the wave direction has shifted to south of the pier, and two rip current features can be seen in the sum image right of the pier. Time sequences of this figure show dynamical changes in the shore-normal features, supporting their source as rip current induced.

just offshore mirrors the bar height, and a brightness gap in the bar image corresponding to a bathymetric minimum, or channel, is seen to be at the source of the second rip current feature, as one expects.

III. PROCESSING NON-COHERENT RADAR IMAGES, ESTABLISHING AN MTF

3D-FFT processing of Window Sequences

The following discussion is a description of the automated sequence of calculations that are done to determine the ISR standard product output at a period chosen by the user for real-time operation. A group of batch files and a task scheduler for Windows XP run both the data acquisition and analysis accordingly. The results are used to discuss difficulties with establishing a meaningful, robust MTF for wave height retrieval using such an approach. While feasible, but troublesome, the data with such caveats are obviously still useful for the modest cost of such a system. However, for equivalent cost, a coherent radar offers an accurate measure of ocean wave directional spectra, with angular resolution better than in-situ sources.

In Figure 1 above was shown standard product output. The red window position is user-selectable, by choosing an azimuth and % total range coverage to place the center of the FFT analysis window. Using 0-deg as the direction to the right from center image, one chooses an angle less than 90 deg, which places the window to the north of the pier. However, to maximize the modulation, and minimize azimuthal dependency of such modulation, a prime direction is chosen based on mean echo strength across the image. The mean echo is calculated over a pie-slice area set by the user, either side of the pier in this case, for example, between 60-80 deg and 100-120 deg. The larger mean value of this pair always tracks the direction of the incoming long wave pattern, and thus assures stronger and consistent modulation. The window location was chosen as 70 deg, with an increment chosen of 40 deg, as the step to use based on the mean calculation either side of the pier, so the window in this case will lie 20 deg either side of it. These positioning variables are left to the user in case unusual coastal features occur in the data that need to be

excluded from both mean value calculation and window placement. The position need not be symmetric about any one direction, and a choice of two prime azimuthal areas is thus established.

A sequence of 512 rotations, 8 sets of 64, are collected with a 1.25-s rotation period, taking ~10 minutes. 40 seconds. 3D-FFT's are performed on the 8 sets of 64, resulting in 32 positive frequency K_x, K_y mean spectra, and 12 of these are user selectable for the real-time display. The 32 negative spectra are mirror images of the positive.

MTF Determination by Comparison with Directional Spectra Surface Truth

For each of the 32 spectra, three peaks are found in order to deal with multi-modal spectra, and the sum of pixel energy at the peak 1 or 2 samples (user selectable) surrounding each peak is used to determine spectral energy content. To determine the MTF, comparison is made with a local surface truth frequency spectrum. As the frequency sampling of the two data sets may not be the same, the surface truth frequency spectrum is typically resampled and interpolated to the same frequencies of the radar analysis.

A plot of radar power samples thus derived is shown plotted in Fig. 3 versus spectral power determined from the frequency spectrum provided by the USACE FRF linear pressure array in 8-m depth of water. This lies at the same offshore distance as the center of the radar window shown in Fig. 1 above. A straight line has been drawn through the data in Fig.3, attempting a fit to the high pressure-sensor samples, as the spread in the lower power region is quite broad. These results show the difficulty in determining a meaningful MTF that will hold over all conditions. The data are sorted by color according to wind speed bands shown on the lower right.

The first set of outliers to address are those green high values occurring in the –10 dB m^2/Hz region, clearly above the linear fit to the higher data samples. These were found to occur while offshore winds were blowing into waves traveling onto shore. The small-scale roughness on the front face of the waves was rougher than occurs when the winds blow in the same direction of the waves, for which most of the data were collected, causing stronger modulation. The second effect is the broad spread in the radar echo for low wind speeds, the red and black samples showing very small radar spectral power. For light offshore winds, upwelling typically occurs, forcing a colder surface than air, and the stability changes markedly, suppresses small-scale roughness. Even with onshore winds at lower speeds, the radar echo becomes a much noisier variable than for higher winds, complicating a valid MTF for such conditions.

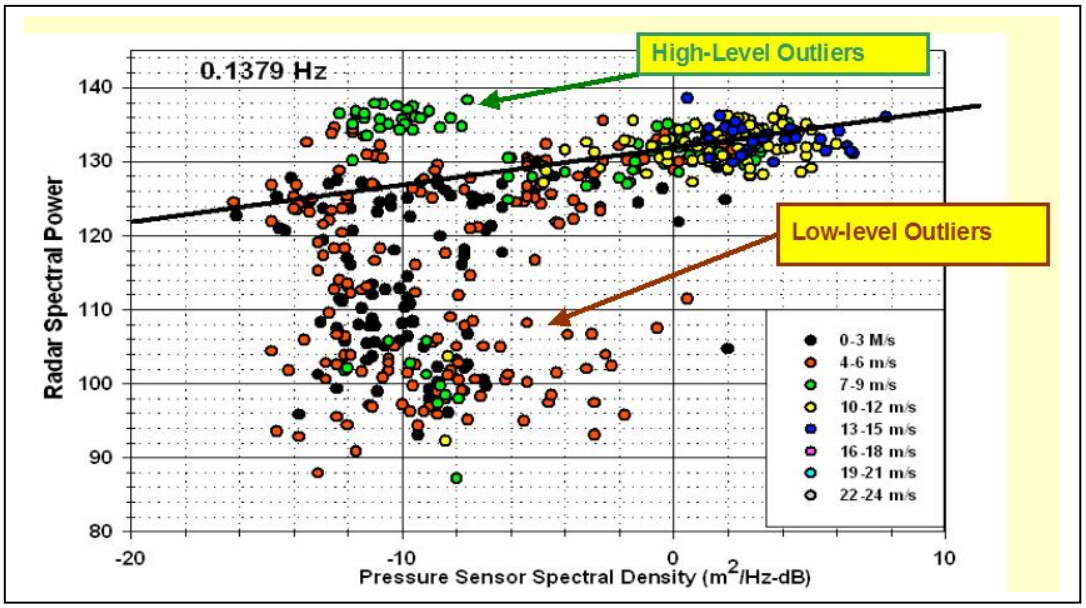

Fig. 3. Radar spectral power vs. pressure sensor spectral power, showing outliers that complicates MTF estimation.

III. COHERENT RADAR AND ORBITAL WAVE MOTION AS A WAVEHEIGHT MEASURE

Description of Fully Coherent and Coherent-on-Receive Marine Radar

A coherent radar provides additional information that can be used to overcome some of these deficiencies. The coherent radar differs from the non-coherent radar in that the phase of the transmitted pulse is fixed from pulse to pulse, while the latter has a phase that is random. Since this phase information is not useful for a standard marine radar, only the echo intensity is available for analysis as presented in the output video signal. The phase information is contained in the bi-polar intermediate frequency (IF) signal, which is normally square-law detected to generate the video signal. This IF signal provides the information necessary to generate signal phase, ϕ, and thus phase differences, $\delta\phi$, from one pulse to the next, which is related to the line-of-sight component radial velocity of the scatterer, dv, by the relation:

$$dv = \delta\phi/\tau * (\lambda/2) \qquad (1)$$

where τ is the time between consecutive radar pulses, λ is the radar wavelength, ~ 3.2 cm for X-band marine radars operating at around 9.4 GHz.

The IF signal from a non-coherent marine radar can be made useful for phase differencing estimates of velocity if one records the phase of the transmitted signal to allow adjustment or relative phase comparison to generate an absolute phase estimate. This approach is known as coherent-on-receive.

A fully coherent radar is a more complex design than a standard marine radar, in that the waveform must be generated by the user, phase-locked oscillators must be used for frequency stability, and a coherent power amplifier must be used in place of non-coherent magnetron sources. Magnetrons serve as both the source and amplifier, in that they respond similar to a bell sounding when hit with an impulse function, generating a very large amplitude output, but with random phase. The coherent high power amplifier (HPA) one the other hand provides a linear amplification of the user waveform input at low levels. They can be quite expensive for long-range detection applications, (traveling-wave-tube, TWT, in the multi-kilowatt output and tens of kilo-dollar price range). However, a much lower power HPA can be used for short range remote sensing applications with price in the range of $10,000 or less. As the signal is coherent, and the waveform is generated by the user, one can make use of pulse compression technology to increase the effective power output by a factor of 1,000 quite easily. See our companion paper for more details [1].

Some Results for a Coherent-on-Receive Radar

As described in a companion paper [1], coherent radars allow the determination of radial velocity image maps, which offer a more quantitative approach to retrieving wave height spectra than the MTF approach described above. Fig. 4 shows a range-azimuth map of radar images in raw form, range vs. waveform # (or azimuth). Images such as these must be transformed to Cartesian co-ordinates by interpolation to produce the type of images shown earlier.

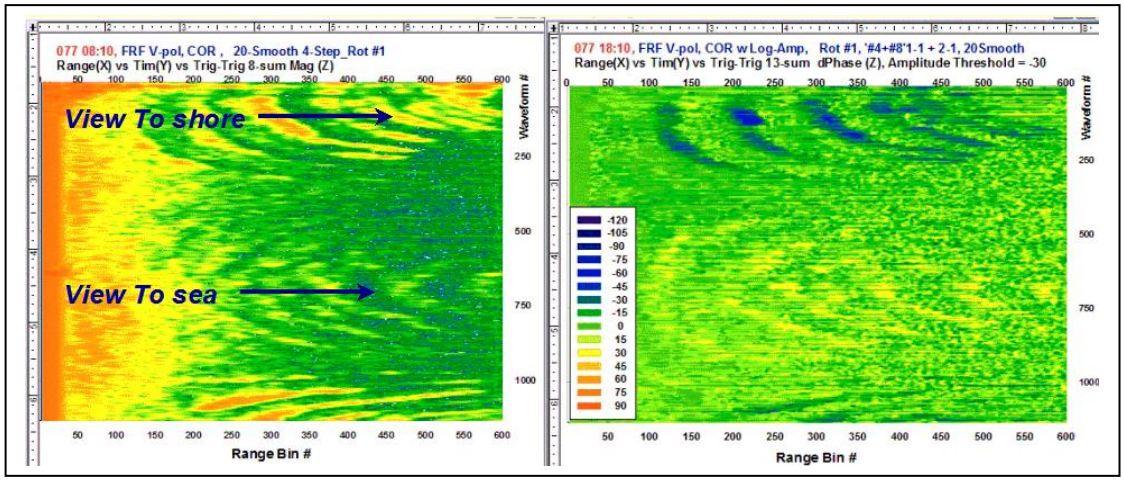

Fig. 4. On the left is shown a range-azimuth (1152 waveforms/350 deg) display of received power for a rotating antenna with the same location and illumination geometry as earlier figures. On the right is shown the corresponding phase difference model derived from the IF signal recorded at the same time, with positive/negative phase difference corresponding to approaching/receding waves. At the top, with a view to shore the wave crests recede and are blue, while midway, 180 deg away and out to sea, the wave crests are approaching and are yellow.

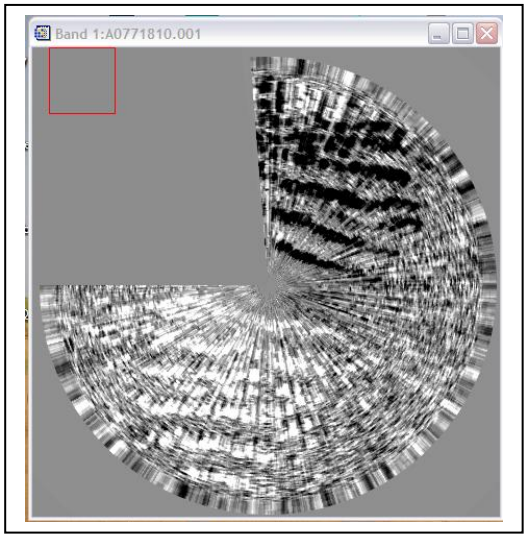

Fig. 5. Cartesian transformed phase-difference imagery from Fig. 4, with brighter pixels representing approaching waves, and darker pixels representing receding waves. A 64 x 64 pixel windows was chosen for 3D-FFT sequence processing.

Transforming the phase difference image on the right in Fig. 4 to Cartesian co-ordinates, one achieves an image similar to those shown in Figs. 1 and 2, but somewhat noisier, shown above in Fig. 5 in gray scale. Brighter pixels are positive radial velocity, and darker pixels are receding. The image is somewhat noisier than the corresponding intensity image, with radial spikes that reflect some temporal modulation of the IF signal, but which does not frequency components that will have an effect on the spatial Fourier transform of a portion of the image. The corresponding K-spectra are below in Fig. 6 from a time series of windows.

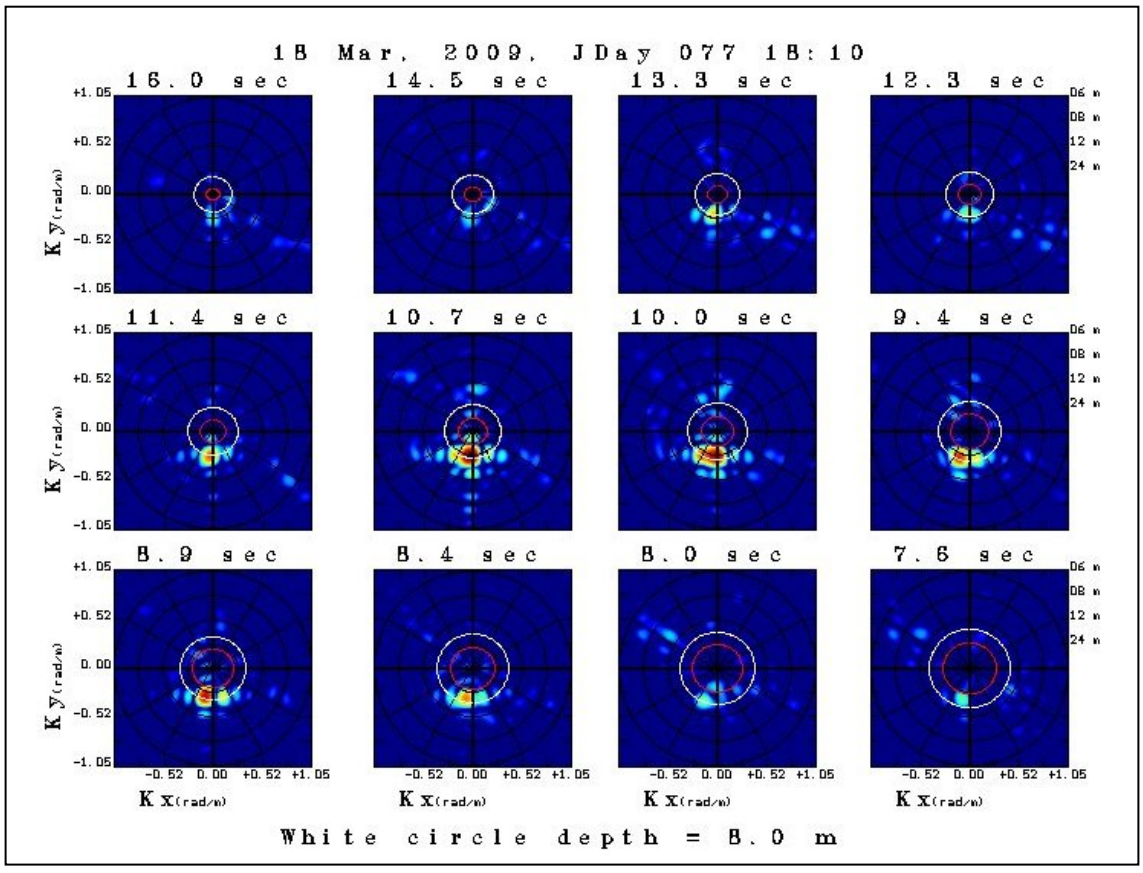

Fig. 6. Radial velocity spectra are derived from a time sequence of images similar to Fig. 5, for a location offshore of the pier as before, in 8-m depth. These results can now be scaled to ocean wave spectral amplitudes directly without the need for application of any modulation transfer function.

The value of wave height can now be derived directly from these radial velocity image spectra using the same tools used for Figs. 1 and 2. To do so, one needs to develop the relation between the orbital wave velocity measurement and wave height. One first writes the value for the horizontal position of a surface particle of surface water moving in sinusoidal motion. Assuming no drift current, a particle on the water surface moves in a circle, with the horizontal position (~ radial position for low grazing angle) given by:

$$X(t) = (H/2)\sin(\Omega t) \tag{2}$$

with corresponding time derivative and horizontal velocity component:

$$dX/dt = \Omega * (H/2)\cos(\Omega t) \tag{3}$$

From Eq. 2, for each spectral component of the 3D Fourier Transform of radial velocity, proportional to $<dX/dt>^2$, a wave height spectral component is derived $<H/2>^2$, without any MTF applied. (Comparisons of results from the FRF pressure array and coherent radar results will be given at the conference presentation.)

Deterministic Wave Profiles from Phase-Difference Imagery

Applications to measurement of ocean wave height maps are straightforward using a coherent radar. Using marine radar, there are approaches that take some 2^N rotations of radar echo intensity imagery, apply the 3D-FFT to sub-windows, scale the spectral results using MTF's, then inverse 3D-FFT the height spectra to derive a wave height map. These methods take at a minimum of 32 rotations of the antenna to produce a real-time wave height map, and are sensitive to the vagaries of MTF estimation as discussed above.

Instead, data such as presented on the right panel of Fig. 4 can be used to provide an immediate spatial wave height map in real time to a good approximation. As the wave frequency spectrum grows with wave frequency as Ω^4 to Ω^5, depending on fetch, wave age, etc, the wave profiles are dominated by the longest wave in the spectrum. Thus, one need only get an estimate of mean wavelength of the longest waves, determine the wave frequency from the deep or shallow water dispersion rule, and then used Eq. 3 to derive H/2 directly using the radial velocity measure, dX/dt, and the corresponding wave frequency estimated. Transformation to Cartesian co-ordinates is not required, as this is typically needed for standard 3D-FFT algorithms as discussed above. One can take the raw radial velocity data in range-azimuth co-ordinates to use in applications such as ship motion response, and do so in nearly real time.

IV. SUMMARY

A description was given of the ISR approach to deriving ocean wave height spectra from time-sequential radar echo images of ocean waves. To derive wave height, one must empirically determine the modulation transfer scaling function, for each frequency component separately, from radar image spectra to wave height spectra using an independent source of directional ocean wave spectra. This requires a minimum of 32 antenna rotations for real time application, and more typically 8 sets of 64 rotations for a robust result that accommodates wave groupiness for stable directional wave spectra. The difficulties of establishing a robust MTF were discussed, with an example of outlying data due to winds blowing opposite the wave direction, causing an enhanced radar echo and modulation, and an incorrect MTF estimate.

Examples of coherent-on-receive phase-difference (~ radial velocity) imagery, derived from the IF signal of a standard marine radar, were used to produce wave number spectra using a similar approach, that obviates the need for an MTF scaling. Wave height spectra are directly retrievable from phase-difference image spectra without such scaling. A discussion was presented that would allow one to determine wave height profiles using a single image for a short term navigation response to local waves, with the assumption that the local wave profile was dominated by the longest spectral component. For predictive models that require a true wave profile over an area, or a complex phase preserving spectrum, the 3D-FFT approach would be necessary, as the scaling between wave height and orbital wave motion depends on an association with a given wave length. However, the vagaries of MTF behavior with environmental variables would no longer be an issue using phase-difference data.

The conference presentation will contain more quantitative comparisons between radar derived wave spectra and in situ directional wave spectra derived from the USACE FRF linear pressure array. ISR is currently in the planning stage for design modifications of our Quadrec recording and processing card to

allow the output of phase-difference and amplitude time series directly in real time, to enhance operational utilization of the approach we have outlined, to be used for wave height field determination.

ACKNOWLEDGMENT

The author wishes to acknowledge the support and cooperation of the U.S. Army Corps of Engineers Field Research Facility and staff for their continued support in the development of ISR remote sensing systems, through a Cooperative Research and Development Agreement between the two parties.

REFERENCES

1. D. Trizna, “Coherent Microwave Marine Radars for Deterministic Wave Profile Mapping, Decameter Scale Coastal Current Mapping, and Ocean Wave Spectrum Measurements”, Proceedings Oceans 2009, Biloxi, 26-29 October 2009.
2. J. Borge, “Use of Conventional Marine Radars to Detect Individual Wave Features in Nearly Real Time”, ONR Workshop on Deterministic Measurement/Simulation of Ocean Waves, Delft, 4-6 May 2009.
3. J. Dannenberg, “WaMos II: Deriving Wave Profiles from X-Band Radar”, ONR Workshop on Deterministic Measurement/Simulation of Ocean Waves, Delft, 4-6 May 2009.
4. E. Thornhill, “Experiences at DRDC with Wave Measurement and Analysis”, ONR Workshop on Deterministic Measurement/Simulation of Ocean Waves, Delft, 4-6 May 2009.